J Physiol (2003), **546.1**, *pp.* 175–189

DOI: 10.1113/jphysiol.2002.029959
www.jphysiol.org

Journal of Physiology

Amplification of exocytosis by Ca^{2+}-induced Ca^{2+} release in INS-1 pancreatic β cells

Guoxin Kang and George G. Holz

Department of Physiology and Neuroscience, New York University School of Medicine, New York, NY 10016, USA

Functional coupling between Ca^{2+}-induced Ca^{2+} release (CICR) and quantal exocytosis in 5-hydroxytryptamine-loaded INS-1 β cells was assessed through the use of carbon fibre amperometry in combination with Fura-2. CICR was evoked by the glucagon-like-peptide-1 (GLP-1) receptor agonist exendin-4 (Ex-4) and was accompanied by quantal secretory events appearing as amperometric current spikes time-locked to the increase of $[Ca^{2+}]_i$. The action of Ex-4 was reproduced by treatment with caffeine, and the source of Ca^{2+} serving as a stimulus for exocytosis originated from ryanodine and thapsigargin-sensitive Ca^{2+} stores. Two distinct patterns of exocytosis occurred within 5 s following the initiation of CICR. Non-summating exocytosis (NS-type) was defined as multiple asynchronous current spikes, and the half-height duration of each spike was 12–48 ms. Summating exocytosis (S-type) was defined as a cluster of spikes. It generated a macroscopic current, the half-height duration of which was 243–682 ms. The release charge of S-type exocytosis was 3.2-fold greater than that of NS-type when measured 2 s following the initiation of secretion. NS-type exocytosis was observed frequently under conditions in which the basal Ca^{2+} concentration ($[Ca^{2+}]_B$) was low (75–150 nM), whereas S-type exocytosis predominated under conditions in which the $[Ca^{2+}]_B$ was elevated (200–275 nM). Depolarization-induced Ca^{2+} influx triggered NS-type exocytosis in most cells tested, irrespective of $[Ca^{2+}]_B$. It is concluded that CICR is a highly effective stimulus for exocytosis in INS-1 cells. The increase of $[Ca^{2+}]_i$ that accompanies CICR stimulates the asynchronous release of a small number of secretory granules under conditions of low $[Ca^{2+}]_B$. When $[Ca^{2+}]_B$ is slightly elevated, CICR targets a much larger pool of secretory granules that undergo summating exocytosis. The transition from NS-type to S-type exocytosis may represent an amplification mechanism for Ca^{2+}-dependent exocytosis.

(Resubmitted 31 July 2002; accepted after revision 16 October 2002; first published online 15 November 2002)
Corresponding author G. G. Holz: Department of Physiology and Neuroscience, Medical Sciences Building Room 442, 550 First Avenue, New York, NY 10016, USA. Email: holzg01@popmail.med.nyu.edu

Insulin is secreted from pancreatic β cells in response to nutrient, hormonal or neural stimuli, and exocytosis of insulin is triggered by the influx of Ca^{2+} through voltage-dependent Ca^{2+} channels (VDCCs; Henquin, 2000). Less well understood is what role the intracellular Ca^{2+} stores play as determinants of β-cell stimulus–secretion coupling. Ca^{2+} is sequestered in the endoplasmic reticulum (ER) as well as in the mitochondria, and significant quantities of Ca^{2+} are also found in the insulin-containing secretory granules (Wollheim & Sharp, 1981; Prentki & Matschinsky, 1987). To what extent Ca^{2+} derived from these various subcellular compartments plays an active role in the stimulation of insulin secretion is a matter of debate. It is clear that exocytosis of insulin is triggered by acetylcholine as a consequence of the mobilization of Ca^{2+} from inositol-trisphosphate-sensitive Ca^{2+} stores (Gromada *et al.* 1999; Gilon & Henquin 2001). Evidence also exists indicating a coupling between nitric-oxide-sensitive Ca^{2+} stores and insulin secretion (Willmott *et al.* 1995), whereas insulin itself is reported to stimulate insulin secretion as a consequence of ER Ca^{2+} mobilization (Xu *et al.* 1999). An as yet to be identified source of intracellular Ca^{2+} is mobilized by the local anaesthetic tetracaine, and Ca^{2+} mobilized in this manner stimulates insulin secretion, an effect not blocked by inhibitors of ER Ca^{2+} sequestration (Bordin *et al.* 1997; Mears *et al.* 1999; Bosqueiro *et al.* 2000).

Studies of β cells or β cell lines (Islam *et al.* 1992, 1998; Leech *et al.* 1994; Chen *et al.* 1996; Gamberucci *et al.* 1999; Holz *et al.* 1999; Kang *et al.* 2001*a*; Lemmens *et al.* 2001) offer support for the existence of a source of Ca^{2+} that is mobilized as a consequence of Ca^{2+}-induced Ca^{2+} release (CICR) from caffeine and ryanodine-sensitive Ca^{2+} stores. CICR is also triggered by the blood-glucose-lowering hormone glucagon-like peptide-1-(7–36)-amide (GLP-1), and the action of GLP-1 is mediated by a cAMP-signalling pathway that sensitizes ryanodine receptor (RYR) Ca^{2+}-release channels to the stimulatory effects of cytosolic Ca^{2+} (Gromada *et al.* 1995; Bode *et al.* 1999; Holz *et al.* 1999; Kang *et al.* 2001*a*). Although the source of Ca^{2+} mobilized by GLP-1 remains to be characterized fully, evidence exists

for the participation of Ca^{2+} stored within the ER (Holz *et al.* 1999; Varadi & Rutter 2002), as well as within the secretory granules (Nakagaki *et al.* 2000; Mitchell *et al.* 2001). Such observations prompt speculation that CICR might play an active role in the Ca^{2+}-dependent stimulation of insulin secretion by GLP-1.

To test this hypothesis, we have focused on the INS-1 β cell line (Asfari *et al.* 1992) because an extensive literature exists documenting Ca^{2+} homeostasis and insulin secretion in these cells (Kennedy *et al.* 1996; Pouli *et al.* 1998; Scheenen *et al.* 1998; Maechler *et al.* 1999; Tsuboi *et al.* 2000). INS-1 cells sequester 5-hydroxytryptamine (5-HT) in secretory granules, and the release of 5-HT serves as a useful surrogate marker for insulin secretion (Aspinwall *et al.* 1999). In the report documented here, measurements of $[Ca^{2+}]_i$ were obtained in 5-HT-loaded cells exposed to the GLP-1 receptor agonist exendin-4 (Ex-4) under conditions in which secretion was monitored at the single-cell level using carbon fibre amperometry in combination with Fura-2. We report that CICR is a highly effective stimulus for exocytosis. Furthermore, the efficacy of CICR as a stimulus for exocytosis is determined by the basal Ca^{2+} concentration ($[Ca^{2+}]_B$). A low $[Ca^{2+}]_B$ favours a small secretory response, whereas elevated $[Ca^{2+}]_B$ allows CICR to recruit a much larger number of secretory granules into the release process. Some of these findings relating to the amplification of exocytosis by CICR have been reported in preliminary form (Kang & Holz 2000, 2002; Kang *et al.* 2001*b*).

METHODS

Cell culture

Rat INS-1 cells (passages 70–90) were cultured as described previously (Asfari *et al.* 1992). Cultures were maintained in a humidified incubator (95 % air–5 % CO_2) at 37 °C in RPMI 1640 medium containing 10 mM Hepes, 11.1 mM glucose, 10 % fetal bovine serum (FBS), 100 U ml^{-1} penicillin G, 100 μg ml^{-1} streptomycin, 2.0 mM L-glutamine, 1.0 mM sodium pyruvate and 50 μM 2-mercaptoethanol. INS-1 cells were passaged by trypsinization and subcultured once a week. Cell suspensions were plated onto glass coverslips (25CIR-1; Fisher Scientific) coated with 1 mg ml^{-1} concanavalin A (type V; Sigma), which facilitates the adherence of cells to glass surfaces. The cell cultures were equilibrated for 16–48 h under these conditions prior to performing the assays illustrated. All reagents for cell culture were obtained from Life Technologies (Rockville, MD, USA).

Measurement of $[Ca^{2+}]_i$

The Fura-2 loading solution consisted of standard extracellular saline (SES) containing (mM): 138 NaCl, 5.6 KCl, 2.6 $CaCl_2$, 1.2 $MgCl_2$, 10 Hepes, and 11.1 D-glucose. The pH was adjusted to 7.35 with NaOH and the osmolarity was adjusted to 295 mosmol using water. The SES was supplemented with 1 μM Fura-2 acetoxymethyl ester (Fura-2 AM; Molecular Probes, Eugene, OR, USA), 2 % FBS and 0.02 % Pluronic F-127 (w/v; Molecular Probes). Cells were exposed to the Fura-2 AM-containing solution for 20–30 min at 22 °C. The loading solution was then removed and the cells were equilibrated in fresh SES for 10 min at 22 °C. Experiments were performed at 32 °C using an Eclipse TE300 inverted microscope (Nikon, Melville, NY, USA) outfitted with a temperature-controlled stage (Medical Systems, Greenvale, NY, USA), a superfusion system and a × 100 Nikon UVF oil-immersion objective (NA 1.3). Dual excitation wavelength microfluorimetry was performed ratiometrically at 0.5 s intervals using a digital video imaging system outfitted with an intensified CCD camera (IonOptix, Milton, MA, USA). A rotating chopper mirror delivered excitation light at 340 or 380 nm, and emitted light was measured at 510 nm. An average of five video frames of imaging data was used to calculate numerator and denominator values for determination of 340/380 ratio values. The $[Ca^{2+}]_i$ was calculated according to the method of Grynkiewicz *et al.* (1985):

$$[Ca^{2+}]_i = K_d \beta\, [(R - R_{min})/(R_{max} - R)],$$

where R is the experimentally derived fluorescence ratio, and R_{min} and R_{max} are ratios measured using calibration solutions containing no Ca^{2+} or saturating Ca^{2+}, respectively. K_d is the dissociation constant (224 nM) describing the interaction of Fura-2 and Ca^{2+}, and β is the fluorescence ratio of free:bound Fura-2 measured with 380 nm excitation.

Calibration of $[Ca^{2+}]_i$

The value of $[Ca^{2+}]_i$ was calculated on the basis of calibration constants determined by *in vitro* and *in vivo* procedures. Calibration of the raw fluorescence values was performed *in vitro* using a Fura-2 pentapotassium salt dissolved in calibration buffers from Molecular Probes (Calcium Calibration Kit 1 with Mg^{2+}). Values of R_{min} and R_{max} were 0.20 and 7.70, respectively, for the experiments described. For the *in vivo* calibration, cells were loaded with Fura-2-AM and exposed to the Ca^{2+} ionophore 4-Br-A23187 (50 μM). Values of R_{min} and R_{max} determined in this manner were 0.22 and 5.1, respectively, under conditions in which the extracellular saline was Ca^{2+}-free (10 mM EGTA with no added Ca^{2+}) or contained a saturating concentration (10 mM) of Ca^{2+}, respectively. The value of $[Ca^{2+}]_B$ calculated on the basis of the *in vitro* and *in vivo* calibrations demonstrated their equivalence.

Assessment of Fura-2 compartmentalization and buffering capacity

Since Fura-2 is a Ca^{2+} buffer, the overloading of cells with Fura-2 might be expected to influence the pattern of Ca^{2+}-dependent exocytosis. Furthermore, intracellular compartmentalization of Fura-2 might lead to a spurious estimate of cytosolic Ca^{2+} concentration, thereby complicating any attempt to draw a correlation between $[Ca^{2+}]_B$, CICR amplitude and the pattern of exocytosis. Despite these caveats, we found that the pattern of exocytosis is unlikely to be explained by differential loading of cells with Fura-2. Increasing the duration of Fura-2 loading from 20–30 to 30–40 min did not alter the likelihood of NS-type or S-type exocytosis in cells exhibiting low or high $[Ca^{2+}]_B$, respectively. Furthermore, the extent of compartmentalization, as determined by digitonin permeabilization (Leech *et al.* 1994), was not significantly different for cells exhibiting NS-type or S-type exocytosis (9 ± 2 % and 10 ± 3 %, respectively; n = 10 cells). An *in vivo* calibration of Fura-2 was also performed using cells loaded with Fura-2-AM and exposed to solutions of known Ca^{2+} concentration in the presence of the Ca^{2+} ionophore 4-Br-A23187. Under these conditions, values of R_{min} and R_{max} did not differ significantly when comparing cells in which NS-type (R_{min} = 0.22 ± 0.04, R_{max} = 4.9 ± 0.07) or S-type (R_{min} = 0.27 ± 0.03, R_{max} = 5.0 ± 0.09) exocytosis was observed. Furthermore, as was the case for estimates based on an *in vitro* calibration, the *in vivo* calibration demonstrated that cells exhibiting NS-type exocytosis

possessed relatively low levels of $[Ca^{2+}]_B$ (82–147 nM, mean = 101 ± 9 nM), whereas cells exhibiting S-type exocytosis possessed higher levels of $[Ca^{2+}]_B$ (200–275 nM; mean = 238 ± 41 nM). Finally, the likelihood of NS-type or S-type exocytosis measured at low or elevated $[Ca^{2+}]_B$, respectively, was found to be unaltered when cells were loaded with Fura-4F (Molecular Probes), an analogue of Fura-2 that exhibits a lower affinity for Ca^{2+} (K_d = 770 nM). These findings demonstrate that the two patterns of exocytosis do in fact occur under conditions of low and high $[Ca^{2+}]_B$, respectively. Furthermore, the two patterns of exocytosis are not generated as a consequence of the differential loading of Fura-2, nor do they reflect cell-to-cell differences in the buffering capacity of Fura-2.

Electrochemical detection of exocytosis

Cells were loaded with 5-HT by incubation in culture medium containing 0.6 mM 5-HT and 0.6 mM 5-hydroxytryptophan. 5-HT is sequestered in large dense-core secretory granules by active transport, but it is excluded from the small synaptic vesicle-like structures that do not contain insulin (Ekholm *et al.* 1971; Gylfe, 1977; Lindstrom *et al.* 1980). 5-HT is co-released with insulin in a glucose- and Ca^{2+}-dependent manner (Gylfe, 1978), and the release of 5-HT serves as a surrogate marker for insulin secretion (Smith *et al.* 1995, 1999; Barbosa *et al.* 1998; Takahashi *et al.* 1999; Bokvist *et al.* 2000). Prolonged exposure of β cells to high concentrations of 5-HT can produce toxic effects (Lindstrom *et al.* 1984; Zawalich *et al.* 2001). For this reason, exposure to 5-HT was limited to 4–16 h and the viability of INS-1 cells was confirmed by demonstrating their ability to exhibit an increase of $[Ca^{2+}]_i$ in response to a stepwise increase in glucose concentration. Carbon fibre electrodes for amperometric detection of secreted 5-HT were prepared as described previously (Schulte & Chow, 1996). A +650 mV potential was applied to a 10 μm diameter carbon fibre, the tip of which was placed adjacent to the cell of interest. The distance from the electrode tip to the cell was ~1 μm. An EPC-9 patch-clamp amplifier was used for detection of the amperometric

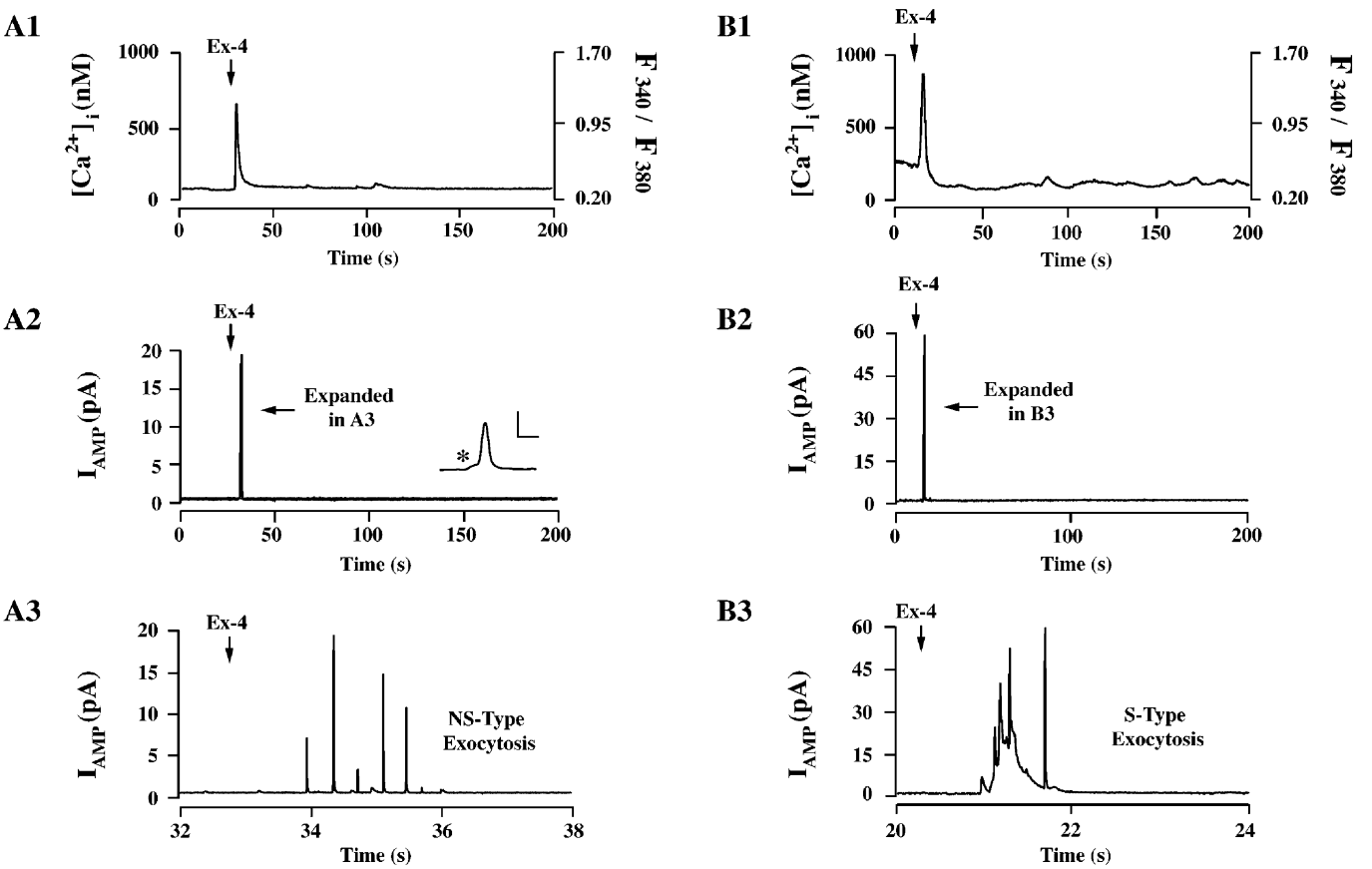

Figure 1. Exendin-4 (Ex-4) triggers Ca^{2+}-induced Ca^{2+} release (CICR) and two distinct patterns of exocytosis

A, application of Ex-4 (10 nM) to a single cell produced CICR (*A1*) and NS-type exocytosis, as depicted on a time scale that is either compressed (*A2*) or expanded (*A3*). Exocytosis was characterized by amperometric current (I_{AMP}) spikes that are time-locked to the increase of $[Ca^{2+}]_i$ (cf. *A1*, *A2*). A current spike of ~25 ms half-height duration is illustrated in the inset of *A2*. It was preceded by a 'foot signal' (asterisk; scale bars 50 ms, 15 pA). *B*, measurements obtained from a second cell in which CICR (*B1*) was accompanied by S-type exocytosis (*B2*, *B3*). The $[Ca^{2+}]_i$ at the start of the experiment was 100 nM for the cell illustrated in *A1–A3*, whereas it was 260 nM for the cell illustrated in *B1–B3*. Vertical arrows in *A* and *B* indicate a 30 s application of Ex-4. In this and all subsequent figures, the amperometric current displayed has been corrected for by subtraction of the leak current (< 5 pA) of the carbon fibre. Variations in the spike amplitude reflect not only the number of secretory granules undergoing exocytosis, but also differential loading of secretory granules with 5-HT. Spike amplitude is also influenced by the distance of the carbon fibre from the site of exocytosis.

current resulting from oxidation of 5-HT. The signal was filtered at 200 Hz, sampled at 1 kHz and stored on a MacIntosh G3 computer running PULSE 8.31 software (Heka, Lambrecht, Germany).

Sources of reagents, reproducibility of findings and preparation of test solutions

Ex-4, caffeine, ryanodine, thapsigargin and 4-Br-A23187 were from Sigma. 8-Br-Rp-cAMPS was from BioLog (Bremen, Germany). Experiments were conducted at least three times to assure reproducibility. Test solutions were dissolved in SES prior to each experiment. For studies examining the effects of Ex-4, the SES contained 0.05% human serum albumin (HSA, fraction V; Sigma) to protect against binding of the peptide to glass or plastic surfaces. No effect of HSA itself was observed. Test solutions were applied to cells from glass micropipettes (type 1B150-6; World Precision Instruments, Sarasota, FL, USA) using a PicoSpritzer II (General Valve, NJ, USA; Holz *et al.* 1993).

Statistical analyses

Population studies were performed using INS-1 cell cultures in which a single coverslip with adherent cells served as the control assay, while a 'sister' culture served as the test assay. A randomly selected sample of 5–10 cells per coverslip was assayed at the single-cell level in order to determine parameters relating to $[Ca^{2+}]_i$, CICR amplitude or the likelihood of NS-type or S-type exocytosis. Each experiment was performed in triplicate and statistical analyses were performed using an analysis of variance combined with the Fisher's PLSD test.

RESULTS

CICR as a stimulus for two distinct patterns of exocytosis

The effect of GLP-1 on Ca^{2+} signalling in β cells is manifest as a fast transient increase of $[Ca^{2+}]_i$ due to the mobilization of Ca^{2+} from intracellular stores. This is followed by a slowly developing and sustained increase of $[Ca^{2+}]_i$ that results from Ca^{2+} influx (Holz *et al.* 1999). INS-1 cells treated with Ex-4 also exhibit these two components of Ca^{2+} signalling, although in the present study we focused only on those cells in which CICR occurred in the absence of the sustained response. INS-1 cells were equilibrated in SES containing 11.1 mM glucose, and test solutions were applied to individual cells via a puffer pipette. Under these conditions, the $[Ca^{2+}]_B$ ranged from 75 to 310 nM (135 ± 65 nM, mean ± S.D.; n = 20 cells), as calculated on the basis of an *in vitro* Fura-2 calibration. This variability of the $[Ca^{2+}]_B$ is a consequence of microheterogeneity, and most likely reflects the dissimilar sensitivities of individual cells to glucose in the extracellular solution (Holz *et al.* 1993).

As reported previously (Kang *et al.* 2001*a*), a 30 s application of the GLP-1 receptor agonist Ex-4 to individual

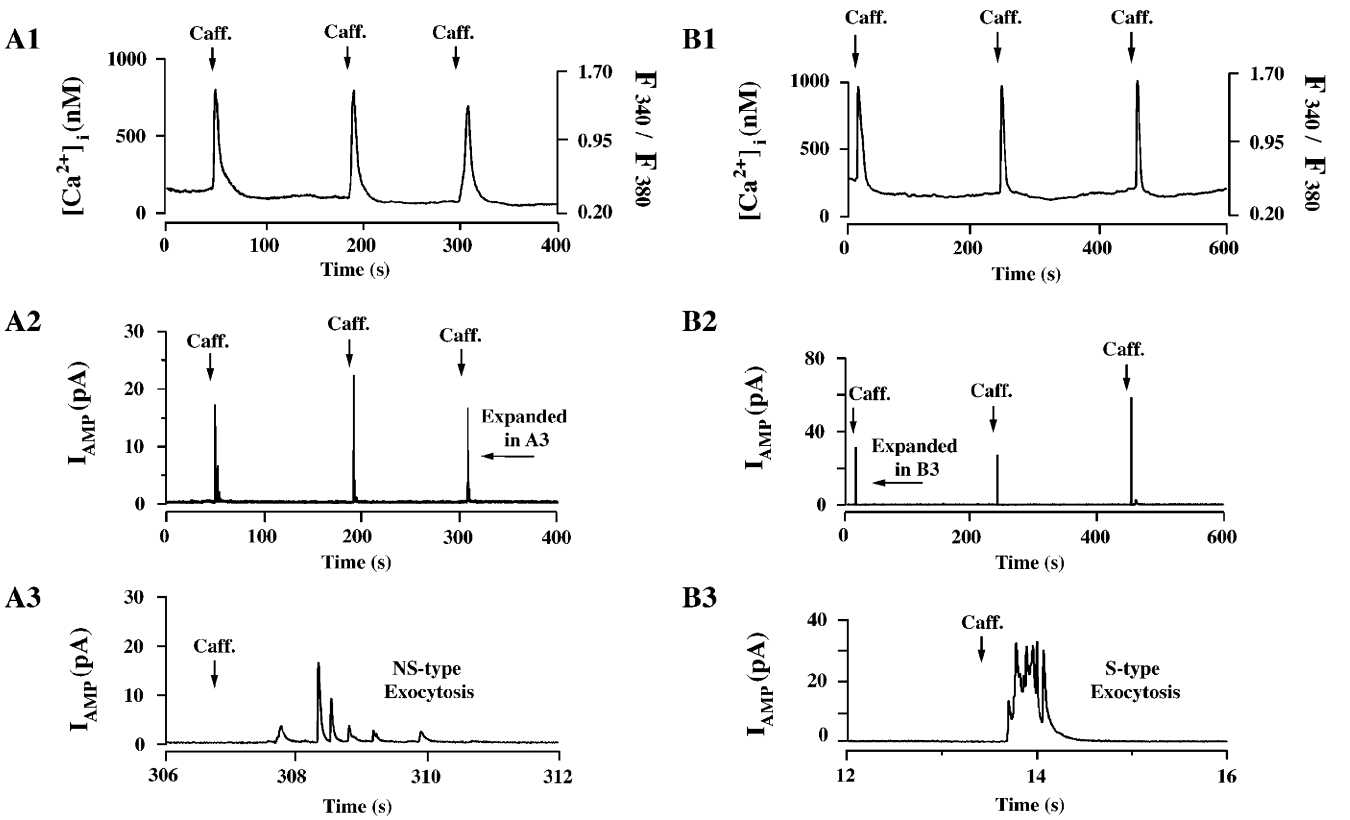

Figure 2. NS-type and S-type exocytosis accompany caffeine-induced CICR

A, application of caffeine (Caff., 10 mM) produced CICR (*A1*) and NS-type exocytosis, here viewed on a compressed (*A2*) or an expanded (*A3*) time scale. *B*, measurements obtained from a second cell demonstrated caffeine-induced CICR (*B1*) and S-type exocytosis (*B2*, *B3*). The $[Ca^{2+}]_i$ at the start of the experiment was 150 nM for the cell illustrated in *A1–A3*, and was 270 nM for the cell illustrated in *B1–B3*. Vertical arrows in *A* and *B* indicate a 30 s application of caffeine using a puffer pipette.

cells produced CICR, which was measured as a fast transient increase of $[Ca^{2+}]_i$ (Fig. 1*A1*). CICR was a stimulus for exocytosis, as evidenced by the appearance of multiple amperometric current spikes that were time-locked to the increase of $[Ca^{2+}]_i$ (Fig. 1*A2*, *A3*). In eight out of 10 cells tested, the $[Ca^{2+}]_B$ was low (75–150 nM, mean 110 ± 27 nM), and CICR was accompanied by a pattern of non-summating exocytosis (Fig. 1*A3*): we defined this as NS-type. NS-type exocytosis exhibited asynchronous current spikes, and the half-height duration of each spike was 12–48 ms. A different pattern of exocytosis (Fig. 1*B1–B3*) accompanied CICR in seven out of 10 cells tested, in which the $[Ca^{2+}]_B$ was elevated (200–275 nM, mean 252 ± 31 nM). We define this summating pattern of exocytosis as S-type because the amperometric current spikes appeared in a synchronous manner and generated a macroscopic current

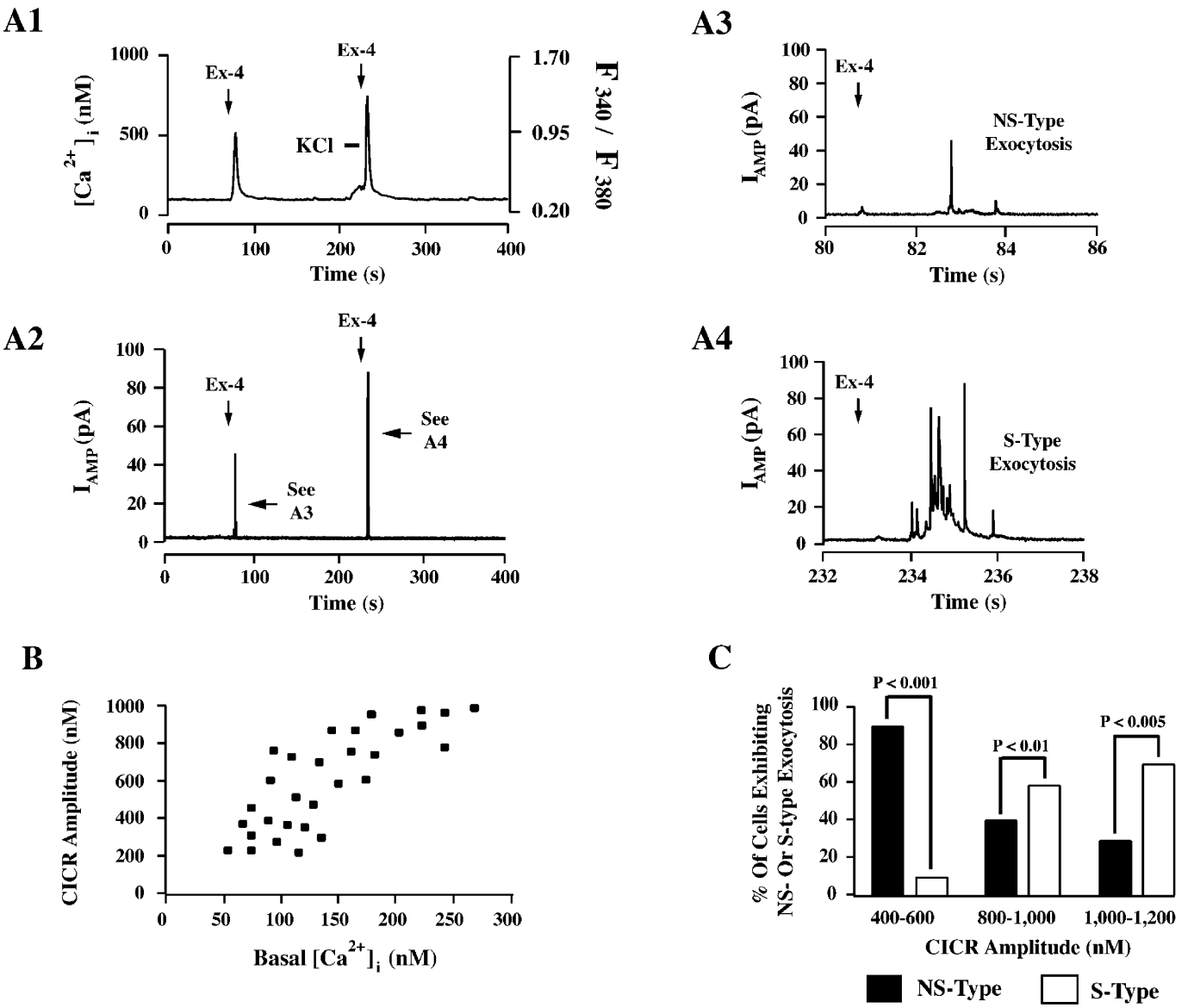

Figure 3. Ca^{2+} dependence of CICR amplitude and exocytosis

A, repeated 30 s applications of Ex-4 produced CICR (*A1*) and exocytosis (*A2*). The pattern of exocytosis accompanying the first application of Ex-4 corresponded to NS-type exocytosis (*A3*) under conditions in which the basal concentration of Ca^{2+} ($[Ca^{2+}]_B$) was 115 nM. $[Ca^{2+}]_B$ was then increased to 203 nM by a 15 s application of standard extracellular saline (SES) containing 28 mM KCl (*A1*). Ex-4 was applied a second time and a pattern of exocytosis corresponding to S-type exocytosis was observed (*A4*). *B*, illustrated is a population study of insulin-secreting (INS)-1 cells (n = 30 cells) demonstrating the positive correlation between $[Ca^{2+}]_B$ and CICR amplitude. Each filled square represents a determination obtained from a single cell exposed to caffeine (10 mM) for 30 s. *C*, NS-type exocytosis in response to caffeine was most frequently observed under conditions of low $[Ca^{2+}]_B$ in which the CICR amplitude was small, whereas S-type exocytosis predominated under conditions of elevated $[Ca^{2+}]_B$ in which the CICR amplitude was large.

spike, the half-height duration of which was 243–682 ms. The increase of $[Ca^{2+}]_i$ that accompanied S-type exocytosis was frequently followed by an undershoot in which the $[Ca^{2+}]_i$ decreased to a value below the initial $[Ca^{2+}]_B$ (Fig. 1*B1*). No exocytosis in response to Ex-4 or caffeine was observed in the absence of CICR.

Properties of exocytosis measured in response to caffeine

The actions of Ex-4 described above were also observed in response to caffeine. Under conditions in which the $[Ca^{2+}]_B$ was low (84–138 nM, mean 112 ± 22 nM), caffeine stimulated CICR (Fig. 2*A1*) and NS-type exocytosis in 19 of 20 cells tested (Fig. 2*A2*, *A3*). In contrast, under conditions in which the $[Ca^{2+}]_B$ was elevated (205–277 nM, mean 256 ± 34 nM), caffeine stimulated S-type exocytosis in 12 of 20 cells tested (Fig. 2*B1–B3*). Therefore, caffeine and Ex-4 exhibited similar actions with respect to the pattern of exocytosis, as well as the Ca^{2+} dependence of exocytosis.

The transition from NS- to S-type exocytosis is correlated with CICR amplitude

A transition from NS-type to S-type exocytosis might represent an amplification mechanism for exocytosis that is itself regulated by the $[Ca^{2+}]_B$. Evidence supporting this concept is provided by our demonstration that the transition from NS-type to S-type exocytosis could be observed in a single cell when the $[Ca^{2+}]_B$ was initially low, but was subsequently elevated by application of a depolarizing concentration of KCl (Fig. 3*A1–A4*). Under these conditions, Ex-4 produced CICR (Fig. 3*A1*), and the amplitude of the Ca^{2+} spike accompanying S-type exocytosis was clearly larger than that accompanying NS-type exocytosis. To evaluate the relationship between $[Ca^{2+}]_B$ and CICR amplitude, a population study of INS-1 cells was conducted. This demonstrated that an increased $[Ca^{2+}]_B$ favoured increased CICR amplitude (Fig. 3*B*). There also existed a positive correlation linking CICR amplitude to the pattern of exocytosis observed. Smaller Ca^{2+} spikes favoured NS-type exocytosis, whereas larger Ca^{2+} spikes were associated with S-type exocytosis (Fig. 3*C*).

Kinetic and statistical comparisons of caffeine-stimulated exocytosis

The properties of NS-type and S-type exocytosis triggered by caffeine were analysed in greater detail using kinetic analysis, whereby the relationship between integrated amperometric current (release charge, Q_{AMP}) and time was determined. NS-type exocytosis (Fig. 4*A*) was compared with S-type exocytosis (Fig. 4*B*), and the Q_{AMP} *versus* time relationship was plotted for the first 2000 ms (t_{2000}) following the start of exocytosis (Fig. 4*C*). This analysis

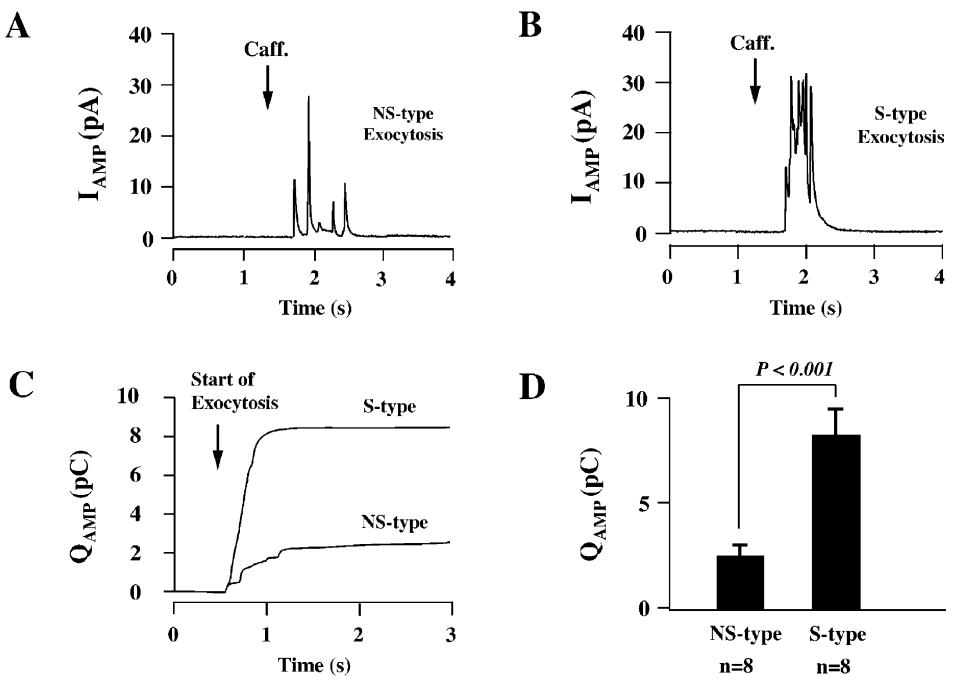

Figure 4. Kinetic analysis of NS-type and S-type exocytosis

NS-type (*A*) and S-type (*B*) exocytosis in response to 10 mM caffeine (30 s) was analysed by determining the integrated amperometric current (or release charge, Q_{AMP}; expressed in pC) *versus* time relationship for each cell (*C*). This revealed the nature of the summation process characteristic of S-type but not NS-type exocytosis. A statistical analysis based on a population study (n = 16 cells) demonstrated that the integrated current measured 2000 ms after initiation of exocytosis differed by a factor of 3.2 for NS-type and S-type exocytosis (*D*). For *C*, the integrated current displayed is that which was calculated after subtraction of the leak current.

revealed that the slope of the Q_{AMP} *versus* time relationship differed for NS-type and S-type exocytosis, as did the plateau value of Q_{AMP} achieved (Fig. 4*C*). On average, the t_{2000} value of Q_{AMP} for S-type exocytosis exceeded by a factor of 3.2 that for NS-type exocytosis (Fig. 4*D*). These findings demonstrate that the amplification of exocytosis observed under conditions of elevated $[Ca^{2+}]_B$ results from an ability of CICR to recruit a releasable pool of secretory granules that is not available for exocytosis at a low $[Ca^{2+}]_B$.

8-Br-Rp-cAMPS fails to alter the pattern of exocytosis

Exocytosis in response to caffeine might result from its direct action to sensitize Ca^{2+} release channels, thereby generating CICR. Alternatively, caffeine might inhibit cAMP-phosphodiesterase (PDE), thereby increasing $[cAMP]_i$ (Islam, 2002). Since cAMP exerts a stimulatory action at the secretory granules (Ammala *et al.* 1993), the inhibition of PDE and the activation of granule-associated protein kinase A (PKA) might explain, at least in part, the stimulation of secretion we observed in response to caffeine. To test for the involvement of PDE, cAMP and PKA in the action of caffeine, cells were pretreated with 8-Br-Rp-cAMPS. This cAMP analogue blocks signal transduction by preventing the interaction between endogenous cAMP and PKA (Botelho *et al.* 1988). A concentration of 200 μM 8-Br-Rp-cAMPS was chosen because it blocks stimulatory actions of cAMP in INS-1 cells (Skoglund *et al.* 2000). 8-Br-Rp-cAMPS failed to block the action of caffeine in our assays of CICR and exocytosis. This was the case when evaluating the ability of caffeine to stimulate NS-type (Fig. 5*A1–A3*) or S-type exocytosis (Fig. 5*B1–B3*). These findings, which are summarized in Table 1, indicate that the effects of caffeine described here are independent of PDE, cAMP and PKA.

We also found that under control conditions, 40 % of cells exhibited CICR in response to Ex-4, whereas only 25 % did so when they were treated with 8-Br-Rp-cAMPS (data not shown). This action of 8-Br-Rp-cAMPS is understandable

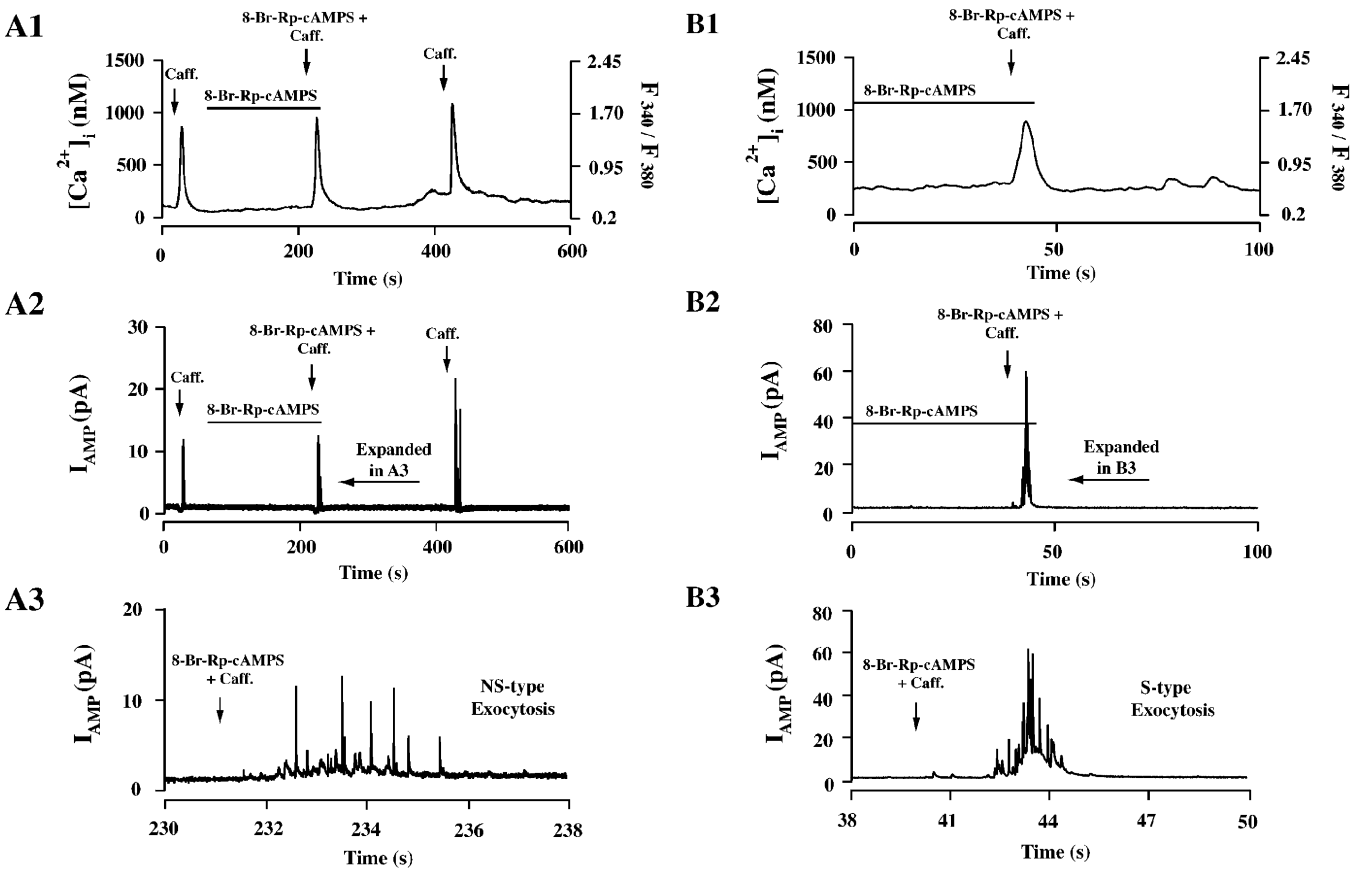

Figure 5. Caffeine-induced exocytosis is not blocked by 8-Br-Rp-cAMPS

A, CICR in response to 10 mM caffeine was independent of phosphodiesterase, cAMP, and protein kinase A because it was not blocked by 200 μM 8-Br-Rp-cAMPS (*A1*). 8-Br-Rp-cAMPS also failed to block NS-type exocytosis in response to caffeine in this same cell (*A2*, *A3*). *B*, the stimulatory action of 10 mM caffeine on CICR (*B1*) and S-type exocytosis (*B2*, *B3*) was not blocked by 200 μM 8-Br-Rp-cAMPS. Vertical arrows indicate a 30 s application of test substances via a puffer pipette. Horizontal bars illustrate the duration of 8-Br-Rp-cAMPS pretreatment prior to application of caffeine.

Table 1. Analysis of the effects of 8-Br-Rp-cAMPS on exocytosis

	Frequency of occurrence for cells exhibiting CICR			
	$[Ca^{2+}]_B$ 75–150 nM		$[Ca^{2+}]_B$ 200–275 nM	
Treatment	NS-Type	S-Type	NS-Type	S-Type
Caffeine	17/20	3/20	8/20	12/20
Caffeine + 8-Br-Rp-cAMPS	11/15	4/15	5/15	10/15
Exendin-4	8/10	2/10	3/10	7/10
Exendin-4 + 8-Br-Rp-cAMPS	7/10	3/10	1/10	9/10

Caffeine (10 mM) and exendin-4 (Ex-4; 10 nM) were administered by local application using puffer pipettes. 8-Br-Rp-cAMPS (200 μM) was added directly to the bath solution and to the test solutions containing caffeine or Ex-4. The two patterns of exocytosis listed are for cells exhibiting Ca^{2+}-induced Ca^{2+} release (CICR). Exocytosis was not observed in the absence of CICR. No significant difference was observed when comparing the likelihood of NS-type or S-type exocytosis in control cells or cells treated with 8-Br-Rp-cAMPS. Findings nearly identical to those presented here were also obtained using Rp-cAMPS in place of 8-Br-Rp-cAMPS. $[Ca^{2+}]_B$ = basal Ca^{2+} concentration.

because unlike caffeine, Ex-4 activates a cAMP signalling pathway (Holz *et al.* 1999; Kang *et al.* 2001*a*). However, in cells that did exhibit CICR, 8-Br-Rp-cAMPS failed to alter the likelihood of NS-type or S-type exocytosis measured at low or high $[Ca^{2+}]_B$ (Table 1). These findings argue that the transition from NS-type to S-type exocytosis is attributable not simply to the actions of cAMP at the secretory granules, but is instead dictated by $[Ca^{2+}]_B$ and CICR amplitude, factors that determine the spatial distribution of Ca^{2+} at the sites of Ca^{2+}-dependent exocytosis.

Emptying of thapsigargin- and ryanodine-sensitive Ca^{2+} stores stimulates exocytosis

Thapsigargin is an inhibitor of sarcoplasmic/endoplasmic reticulum Ca^{2+}-ATPases (SERCA) that mediate Ca^{2+} uptake, and it is used to deplete Ca^{2+} stores in an ER-specific manner. Application of thapsigargin produced an increase of $[Ca^{2+}]_i$ (Fig. 6*A1*) that was time-locked to the appearance of numerous amperometric current spikes (Fig. 6*A2*, *A3*). Under conditions of thapsigargin treatment, caffeine failed to stimulate CICR in most cells tested, and no exocytosis

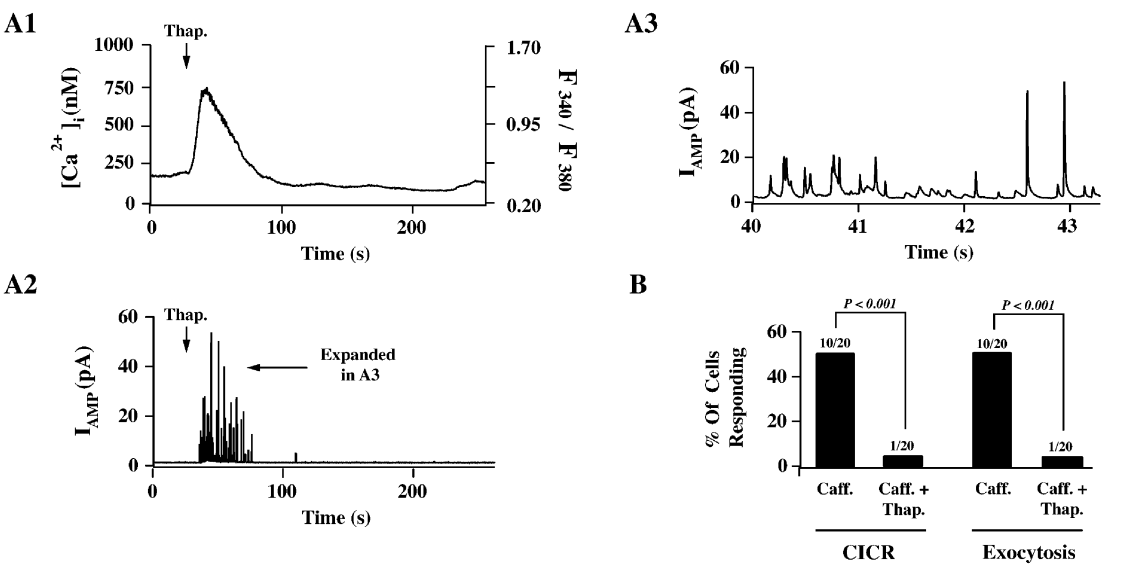

Figure 6. Functional coupling of thapsigargin-sensitive Ca^{2+} stores to exocytosis

A, a 30 s application of 1 μM thapsigargin (Thap.) produced an increase of $[Ca^{2+}]_i$ (*A1*) that was time-locked to the appearance of multiple amperometric current spikes (*A2*). The pattern of exocytosis for this cell is displayed on a compressed (*A2*) or an expanded (*A3*) time scale. *B*, a population study demonstrated that CICR in response to caffeine was blocked by the addition of thapsigargin (1 μM, 5–10 min exposure) to the solution bathing the cells. In these same cells, thapsigargin also blocked the exocytosis that accompanied CICR. Thapsigargin was prepared as a stock solution dissolved in DMSO, and the final concentration of DMSO in the SES was 0.01 % w/v. For cells not treated with thapsigargin, 0.01 % DMSO was included in the bath solution. The number above each bar of the histogram indicates the fraction of cells exhibiting caffeine-induced CICR and exocytosis. For this and all subsequent figures, the criteria used for calculating the percentage of cells exhibiting CICR are the same as those reported previously (Kang *et al.* 2001*a*).

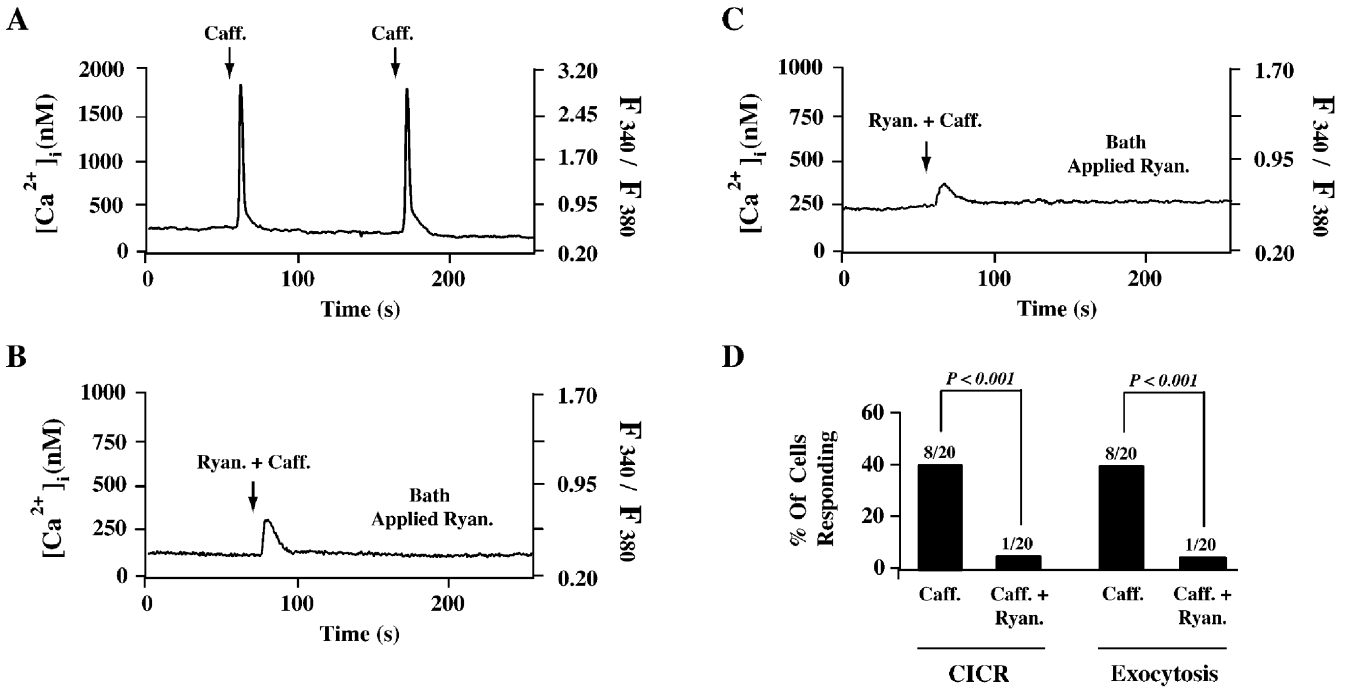

Figure 7. Ryanodine sensitivity of caffeine-induced CICR

A, a 30 s application of 10 mM caffeine (arrows) generated CICR. *B* and *C*, the action of caffeine was blocked by 10 μM ryanodine (Ryan.) added to saline comprising the bath and puffer solutions. Note that the action of ryanodine was measured in cells exhibiting a low (*B*) or elevated (C) $[Ca^{2+}]_B$. In the presence of ryanodine, a small non-regenerative increase of $[Ca^{2+}]_i$ was observed in response to caffeine. These cells were considered not to exhibit CICR according to criteria published previously (Kang *et al.* 2001*a*). *D*, a population study of 20 cells demonstrated that the frequency of occurrence for caffeine-induced CICR and the accompanying exocytosis was reduced by treatment with ryanodine.

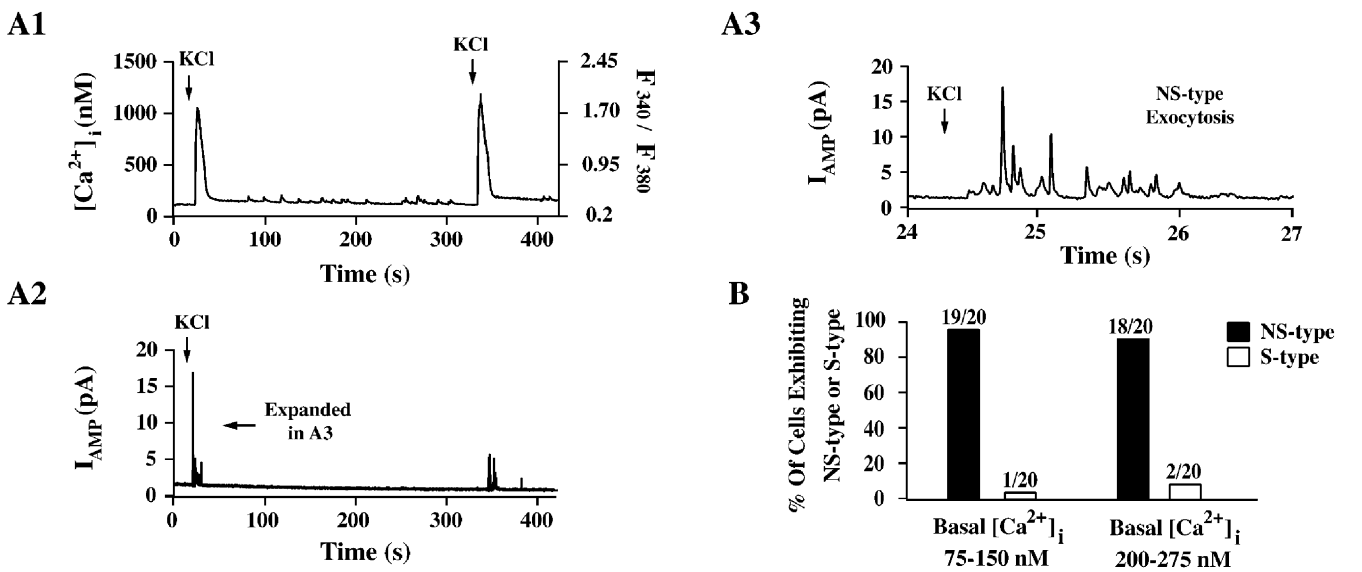

Figure 8. Properties of KCl-induced exocytosis

A, measurements of $[Ca^{2+}]_i$ (*A1*) and NS-type exocytosis, as depicted on a compressed (*A2*) and an expanded (*A3*) time scale, following application of 56 mM KCl (5 s, arrows) via a puffer pipette. The $[Ca^{2+}]_i$ at the start of the experiment was 95 nM. *B*, the predominant pattern of exocytosis measured in response to 56 mM KCl was NS-type exocytosis, not only in cells exhibiting a low $[Ca^{2+}]_B$, but also in cells in which the $[Ca^{2+}]_B$ was elevated. Numbers above each bar of the histogram indicate the fraction of cells exhibiting NS-type or S-type exocytosis.

was observed (Fig. 6*B*). Therefore, caffeine mobilizes Ca^{2+} from thapsigargin-sensitive Ca^{2+} stores, and Ca^{2+} released from these stores acts as a stimulus for exocytosis. Ca^{2+} stores targeted by thapsigargin included those regulated by RYR Ca^{2+}-release channels, because ryanodine inhibited CICR and the exocytosis measured in response to caffeine at low or high $[Ca^{2+}]_B$ (Fig. 7*A–D*).

Ca^{2+} influx as a stimulus for NS-type but not S-type exocytosis

NS-type exocytosis was observed frequently when Ca^{2+} influx through VDCCs was stimulated by application of 56 mM KCl (Fig. 8*A1–A3*). KCl stimulated NS-type exocytosis in nearly all cells tested, whereas S-type exocytosis was observed only infrequently, even under conditions of elevated $[Ca^{2+}]_B$ (Fig. 8*B*). KCl-induced Ca^{2+} influx also failed to trigger S-type exocytosis in cells treated with forskolin in the presence of ryanodine (Fig. 9*A1–A3* and *B1–B3*; note low and high $[Ca^{2+}]_B$, respectively). Under these conditions, CICR was blocked, cAMP production was increased and PKA was activated. Since PKA increases the size of the readily releasable pool (RRP) of secretory granules (Renstrom *et al.* 1997), it may be concluded that S-type exocytosis is CICR-dependent, and can not be explained simply by an increased RRP size. Finally, the kinetic properties of NS-type exocytosis measured in response to KCl (Fig. 10*A*) were compared with those of S-type exocytosis measured in response to caffeine (Fig. 10*B*). Exocytosis differed with respect to the slope of the Q_{AMP} *versus* time relationship as well as the plateau value achieved (Fig. 10*C*). The value of Q_{AMP} measured 2000 ms following the initiation of secretion differed by a factor of 3.6 when comparing NS-type (KCl) and S-type (caffeine) exocytosis (Fig. 10*D*).

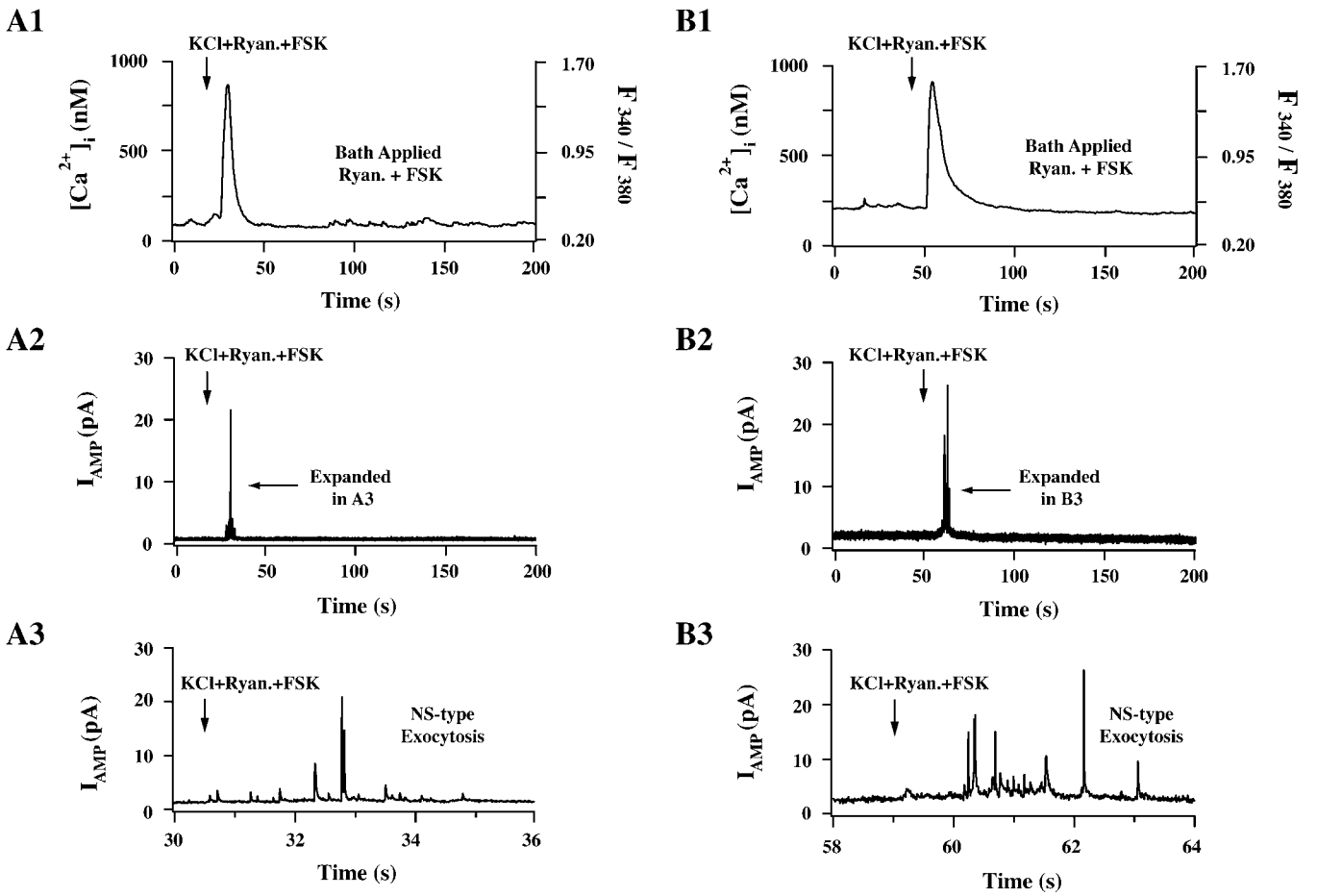

Figure 9. KCl-induced exocytosis in cells treated with forskolin and ryanodine

A, 2 μM forskolin (FSK) and 10 μM ryanodine were added directly to the bath solution so as to elevate cAMP levels while simultaneously suppressing CICR in a cell that exhibited a low $[Ca^{2+}]_B$ at the start of the experiment. Application of 56 mM KCl via a puffer pipette produced an increase of $[Ca^{2+}]_i$ (*A1*) and NS-type exocytosis, as depicted on a compressed (*A2*) or expanded (*A3*) time scale. *B*, an increase of $[Ca^{2+}]_i$ (*B1*) and NS-type exocytosis (*B2*, *B3*) was observed when KCl was applied to a cell in which the $[Ca^{2+}]_B$ was initially elevated. Arrows in *A* and *B* indicate a 5 s application of the test solution containing 56 mM KCl, 2 μM forskolin, and 10 μM ryanodine.

DISCUSSION

Properties of exocytosis triggered by CICR

In the report presented here it is demonstrated that CICR evokes two distinct patterns of exocytosis, which we define as NS-type and S-type exocytosis. Non-summating asynchronous current spikes characterize NS-type exocytosis, whereas S-type exocytosis is manifested as synchronous spikes that exhibit summation, and which generate a macroscopic current. NS-type exocytosis triggered by CICR is observed under conditions in which $[Ca^{2+}]_B$ is low, and it is also observed in response to KCl-induced Ca^{2+} influx. S-type exocytosis is triggered most frequently by CICR and is observed when $[Ca^{2+}]_B$ is elevated. It is rarely observed in response to KCl. On the basis of these observations, we propose that a transition from NS-type to S-type exocytosis represents a CICR-specific amplification mechanism for Ca^{2+}-dependent exocytosis. Although a previous study demonstrated a role for CICR in the amplification of exocytosis at the frog neuromuscular junction (Narita *et al.* 2000), no statement could be made as to how the pattern of exocytosis was altered. We suggest that under conditions of low $[Ca^{2+}]_B$, CICR or KCl-induced depolarization triggers exocytosis that is limited to a small number of secretory granules, many of which discharge their contents in an unsynchronized manner (NS-type exocytosis). In contrast, under conditions of elevated $[Ca^{2+}]_B$, the co-ordinated release of a large number of secretory granules occurs (S-type exocytosis), thereby providing a process of amplification that is CICR-specific.

Factors responsible for the appearance of S-type exocytosis

The two types of exocytosis we describe resemble in some ways the exocytosis observed in mouse β cells (Takahashi *et al.* 1999; Kasai *et al.* 2002). Exocytosis that occurs following the uncaging of caged Ca^{2+} in mouse β cells is characterized by a non-summating pattern of exocytosis that is observed under conditions of low $[ATP]_i$. Increasing the $[ATP]_i$ to 3 mM allows for the appearance of a summating pattern of exocytosis similar to what we define as S-type. At 0.5 mM $[ATP]_i$, cAMP facilitates the summating behaviour. We interpret these prior findings to indicate that cAMP acts directly at the secretory granules to facilitate their

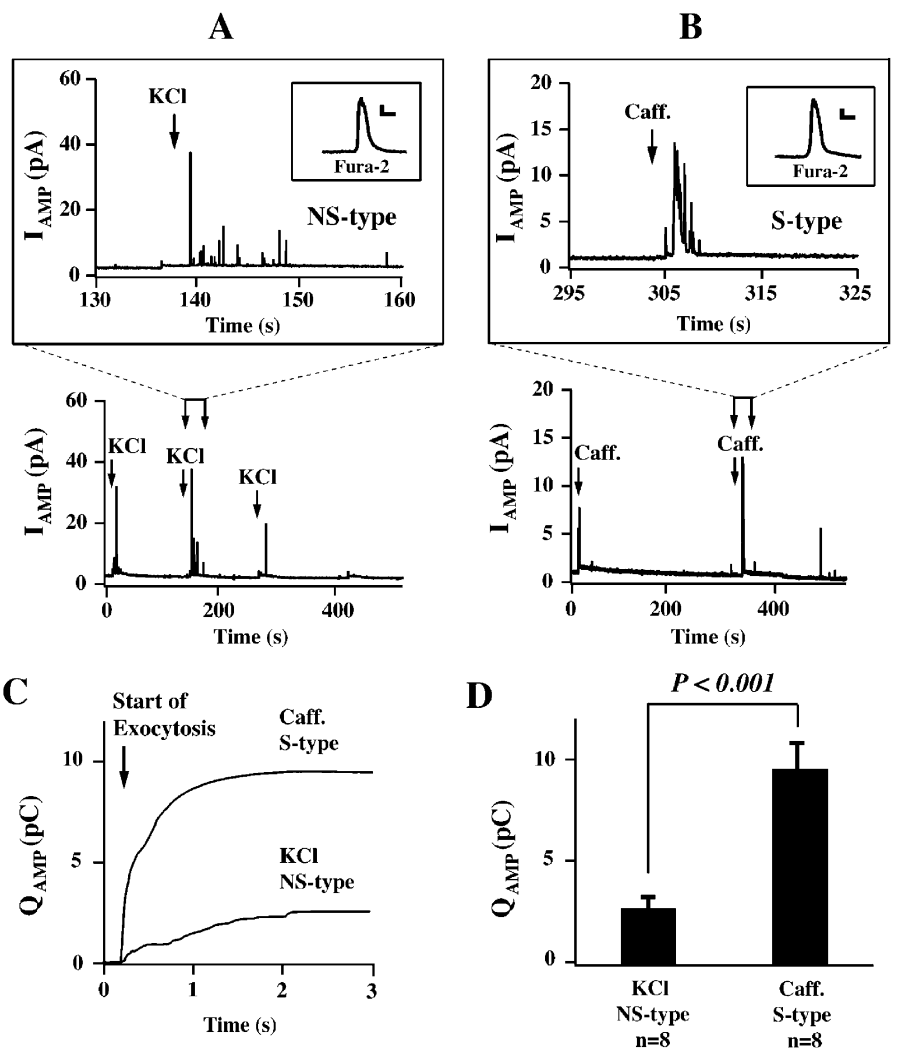

Figure 10. Comparisons of caffeine and KCl-induced exocytosis

A, NS-type exocytosis measured in response to 56 mM KCl, as viewed on an expanded (top) and compressed (bottom) time scale. *B*, S-type exocytosis measured in response to 10 mM caffeine, as viewed on an expanded (top) and compressed (bottom) time scale. The duration of KCl application (5 s) was optimized to produce an increase of $[Ca^{2+}]_i$, the time course and amplitude of which resembled that produced by a 30 s exposure to caffeine (cf. Figs 2*A1* and 8*A1*). The insets of *A* and *B* illustrate the changes of $[Ca^{2}]_i$ that accompanied exocytosis in these two cells. Calibration bars for the insets: vertical 100 nM, horizontal 20 s. *C*, the Q_{AMP} *versus* time relationship was determined for each of the cells illustrated in *A* and *B*. *D*, a population study ($n = 16$ cells) demonstrated that the integrated current measured 2000 ms after initiation of exocytosis differed by a factor of 3.6 for KCl (NS-type) and caffeine (S-type).

release, and that this is the primary means by which S-type exocytosis is triggered under conditions in which Ca^{2+} is not a limiting factor (i.e. when a global increase of $[Ca^{2+}]_i$ is achieved due to the uncaging of caged Ca^{2+}).

It is important to note, however, that such a direct action of cAMP at the secretory granules is unlikely to be the sole means by which S-type exocytosis is initiated. In our own studies, the generation of CICR is a rate-limiting factor for S-type exocytosis because it provides the global increase of $[Ca^{2+}]_i$ necessary for the recruitment of secretory granules into the release process. Indeed, we demonstrate that there exists a positive correlation between elevated $[Ca^{2+}]_B$, increased CICR amplitude and the appearance of S-type exocytosis. Therefore, we propose that S-type exocytosis is a dually regulated process involving the stimulatory effects of cAMP and Ca^{2+} not only at secretory granules, but also at intracellular Ca^{2+}-release channels. The synergism between cAMP and Ca^{2+} that promotes CICR and directly facilitates exocytosis results in the co-ordinated release of a large number of secretory granules, thereby generating the summating behaviour. Such a synergism is suggested by the demonstrated abilities of cAMP and Ca^{2+} to promote the opening of RYR Ca^{2+}-release channels while simultaneously increasing the size of the RRP of secretory granules (von Ruden & Neher 1993; Renstrom *et al.* 1997; Smith *et al.* 1998; Gromada *et al.* 1999; Holz *et al.* 1999; Kang *et al.* 2001*a*).

The pattern of exocytosis is not influenced by 8-Br-Rp-cAMPS

We found that 8-Br-Rp-cAMPS, an inhibitor of PKA activation, failed to alter the likelihood of NS-type or S-type exocytosis in cells that exhibited CICR. We interpret this finding to indicate that under physiological conditions of Ca^{2+} signalling, the pattern of exocytosis is dictated primarily by the availability of Ca^{2+}, not the activity of PKA. This finding is surprising in light of the findings of Takahashi and co-workers that PKA plays an important role in facilitating exocytosis in mouse β cells (Takahashi *et al.* 1999; Kasai *et al.* 2002). It is important to note, however, that INS-1 cells express not only PKA, but also cAMP-regulated guanine nucleotide exchange factors (cAMPGEFs; Leech *et al.* 2000). The cAMPGEFs mediate the stimulatory effects of cAMP on Ca^{2+}-dependent insulin secretion (Ozaki *et al.* 2000; Kashima *et al.* 2001), and they are thought to be important determinants of GLP-1 receptor-mediated signal transduction. Although 8-Br-Rp-cAMPS is an established inhibitor of PKA, its effectiveness at cAMPGEFs is unknown. Recent studies suggest that Rp-cAMPS is a poor antagonist of cAMPGEFs (J. L. Bos, personal communication). It is possible, therefore, that an 8-Br-Rp-cAMPS-insensitive action of cAMP exists at the secretory granules, and that such an action plays some role in determining the likelihood of NS-type or S-type exocytosis.

In this regard, it is noteworthy that previous studies demonstrated cAMP to exert direct stimulatory effects on exocytosis. Slow exocytosis is blocked by Rp-cAMPS. It most likely reflects the PKA-mediated refilling of a RRP (Renstrom *et al.* 1997). Fast exocytosis is insensitive to Rp-cAMPS. It may reflect an increased probability that granules already in the RRP will undergo exocytosis (Renstrom *et al.* 1997). One interpretation of these findings is that the facilitation of fast exocytosis by cAMP reflects its binding to cAMPGEFs, whereas the facilitation of slow exocytosis involves PKA. Should this prove to be the case, our findings are most easily interpreted in terms of a selective action of CICR to trigger fast exocytosis in a cAMPGEF-mediated manner that is insensitive to 8-Br-Rp-cAMPS.

Spatial considerations of Ca^{2+} signalling

Our studies lead us to propose that spatial considerations of Ca^{2+} signalling must be taken into account when considering which factors dictate the pattern of exocytosis. In our model, NS-type exocytosis results from secretion restricted to active zones where a small number of secretory granules release their contents. In contrast, S-type exocytosis may result from secretion occurring not only within, but also outside of active zones where many more secretory granules congregate. Active zones are defined here as regions of the plasma membrane where VDCCs and secretory granules colocalize (Bokvist *et al.* 1995; Qian & Kennedy, 2001). It is well known that Ca^{2+} influx through VDCCs produces an increase of $[Ca^{2+}]_i$ that is restricted to microdomains of the cation located at the inner pore of VDCCs (Llinas *et al.* 1995). These microdomains form at active zones where VDCCs are situated in close proximity to a small number of secretory granules constituting a docked, primed and readily releasable pool (Bokvist *et al.* 1995; Barg *et al.* 2001, 2002). A larger pool of granules is positioned at a distance from the active zones (Pouli *et al.* 1998; Tsuboi *et al.* 2000; Ohara-Imaizumi *et al.* 2002), and for this reason, they are not influenced by the spatially restricted Ca^{2+} signal generated by Ca^{2+} influx.

We propose that the transition from NS-type to S-type exocytosis can be viewed as a cAMP-regulated process that is itself influenced by the prevailing $[Ca^{2+}]_B$. In our model, Ca^{2+} influx through VDCCs triggers NS-type exocytosis under conditions in which $[cAMP]_i$ is low. In the presence of Ex-4, cAMP levels are elevated and sensitization of RYRs allows Ca^{2+} influx to trigger CICR at point sources on the ER located close to the active zones. When $[Ca^{2+}]_B$ is low, ER Ca^{2+} stores are not full and CICR is not fully regenerative. For this reason, CICR is restricted to the active zones where it triggers NS-type exocytosis only. Although cAMP and Ca^{2+} exert direct stimulatory actions at secretory granules found within active zones, the number of granules released is too small to allow for the appearance of S-type exocytosis. Instead, what is predicted

to occur is an increased number of exocytotic events comprising NS-type exocytosis. This explains why KCl-induced depolarization is an ineffective stimulus for S-type exocytosis when cells are treated with forskolin (to increase levels of cAMP) and ryanodine (to block CICR). In contrast, when $[Ca^{2+}]_B$ is elevated, ER Ca^{2+} stores are full, thereby allowing Ca^{2+} influx to trigger regenerative CICR if and only if RYRs are sensitized by Ex-4. Under these conditions, CICR may target a large RRP of 'distant' secretory granules located outside of the active zones, thereby generating S-type exocytosis. A prediction of this model is that NS-type exocytosis will predominate when cells are exposed to glucose in the absence of RYR sensitization. This prediction is substantiated by published findings in which a pattern of exocytosis analogous to NS-type exocytosis was observed after exposure of mouse β cells to a concentration of glucose that produced depolarization and the generation of actions potentials (Bokvist *et al.* 2000).

Physiological significance

Previous studies of isolated islets of Langerhans focused on the action of GLP-1 as a facilitator of the 'triggering pathway' of glucose-dependent insulin secretion. GLP-1 inhibits ATP-sensitive K^+ channels (K-ATP; Holz & Habener 1992; Holz *et al.* 1993), and it augments the L-type Ca^{2+} current while exerting a direct stimulatory action at the secretory granules (Gromada *et al.* 1998*a*, *b*). The findings presented here suggest a novel and previously unrecognized action of GLP-1 that complements these effects by favouring a shift in the pattern of exocytosis. We propose that the small quantities of insulin secreted in a pulsatile manner during the fasting state (between meals) may result from NS-type exocytosis, whereas first-phase insulin secretion occurring during the feeding state may reflect S-type exocytosis. This idea is in keeping with the observation that insulin secretion during the fasting state results, at least in part, from the stimulatory effects of glucose occurring at a low concentration of sugar in the near absence of GLP-1. Ingestion of a meal generates an increase of blood glucose concentration and a rise in the circulating level of GLP-1. It is only then that GLP-1 facilitates the insulin secretagogue action of glucose, thereby producing the incretin hormone effect (Holst, 1997). Elevated concentrations of blood glucose occur during the feeding state, and metabolism of glucose by the β cell produces the inhibition of K-ATP that allows for membrane depolarization and Ca^{2+} influx. In this manner, inhibition of K-ATP provides the increase of β-cell $[Ca^{2+}]_i$ necessary for CICR. Under these conditions, GLP-1 sensitizes the Ca^{2+} release mechanism, thereby allowing for the appearance of S-type exocytosis. In conclusion, we propose that the transition from NS-type to S-type exocytosis may be viewed as a key determinant of first-phase insulin secretion.

REFERENCES

Ammala C, Ashcroft FM & Rorsman P (1993). Calcium-independent potentiation of insulin release by cyclic AMP in single β-cells. *Nature* **363**, 356–358.

Asfari M, Janjic D, Meda P, Li G, Halban PA & Wollheim CB (1992). Establishment of 2 mercaptoethanol-dependent differentiated insulin-secreting cell lines. *Endocrinology* **130**, 167–178.

Aspinwall CA, Huang L, Lakey JR & Kennedy RT (1999). Comparison of amperometric methods for detection of exocytosis from single pancreatic β-cells of different species. *Anal Chem* **71**, 5551–5556.

Barbosa RM, Silva AM, Tome AR, Stamford JA, Santo RM & Rosario LM (1998). Control of pulsatile 5-HT/insulin secretion from single mouse pancreatic islets by intracellular calcium dynamics. *J Physiol* **510**, 135–143.

Barg S, Eliasson L, Renstrom E & Rorsman P (2002). A subset of 50 secretory granules in close contact with L-type Ca^{2+} channels accounts for first-phase insulin secretion in mouse β-cells. *Diabetes* **51**, S74–82.

Barg S, Ma XS, Eliasson L, Galvanovskis J, Gopel SO, Obermuller S, Platzer J, Renstrom E, Trus M, Atlas D, Striessnig J & Rorsman P (2001). Fast exocytosis with few Ca^{2+} channels in insulin-secreting mouse pancreatic B-cells. *Biophys J* **81**, 3308–3323.

Bode HP, Moormann B, Dabew R & Goke B (1999). Glucagon-like peptide-1elevates cytosolic calcium in pancreatic β-cells independently of protein kinase A. *Endocrinology* **140**, 3919–3927.

Bokvist K, Eliasson L, Ammala C, Renstrom E & Rorsman P (1995). Co-localization of L-type Ca^{2+} channels and insulin-containing secretory granules and its significance for the initiation of exocytosis in mouse pancreatic B-cells. *EMBO J* **14**, 50–57.

Bokvist K, Holmqvist M, Gromada J & Rorsman P (2000). Compound exocytosis in voltage clamped mouse pancreatic β-cells revealed by carbon fibre amperometry. *Pflugers Arch* **439**, 634–645.

Bordin S, Carneiro EM, Bosqueiro JR & Boschero AC (1997). Tetracaine stimulates extracellular Ca^{2+} -independent insulin release. *Eur J Pharmacol* **327**, 257–262.

Bosqueiro JR, Carneiro EM, Bordin S & Boschero AC (2000). Tetracaine stimulates insulin secretion through the mobilization of Ca^{2+} from thapsigargin- and IP_3 insensitive Ca^{2+} reservoir in pancreatic β-cells. *Can J Physiol Pharmacol* **78**, 462–468.

Botelho LH, Rothermel JD, Coombs RV & Jastorff B (1988). cAMP analog antagonists of cAMP action. *Methods Enzymol* **159**, 159–172.

Chen TH, Lee B, Yang C & Hsu WH (1996). Effects of caffeine on intracellular Ca^{2+} release and Ca^{2+} influx in a clonal β-cell line RINm5F. *Life Sci* **58**, 983–990.

Ekholm R, Ericson LE & Lundquist I (1971). Monoamines in the pancreatic islets of the mouse. Subcellular localization of 5-hydroxytryptamine by electron microscopic autoradiography. *Diabetologia* **7**, 339–348.

Gamberucci A, Fulceri R, Pralong W, Banhegyi G, Marcolongo P, Watkins SL & Benedetti A (1999). Caffeine releases a glucose-primed endoplasmic reticulum Ca^{2+} pool in the insulin-secreting cell line INS-1. *FEBS Lett* **446**, 309–312.

Gilon P & Henquin JC (2001). Mechanisms and physiological significance of the cholinergic control of pancreatic β-cell function. *Endocr Rev* **22**, 565–604.

Gromada J, Bokvist K, Ding, WG, Holst JJ, Nielsen JH & Rorsman P (1998*a*).Glucagon-like peptide-1-(7–36)-amide stimulates exocytosis in human pancreatic β-cells by both proximal and distal regulatory steps in stimulus-secretion coupling. *Diabetes* **47**, 57–65.

Gromada J, Dissing S, Bokvist K, Renstrom E, Frokjaer-Jensen J, Wulff BS & Rorsman P (1995). Glucagon-like peptide-1 increases cytoplasmic Ca^{2+} in insulin secreting βTC3-cells by enhancement of intracellular Ca^{2+} mobilization. *Diabetes* **44**, 767–774.

Gromada J, Holst JJ & Rorsman P (1998*b*). Cellular regulation of islet hormone secretion by the incretin hormone glucagon-like peptide-1. *Pflugers Arch* **435**, 583–594.

Gromada J, Hoy M, Renstrom E, Bokvist K, Eliasson L, Gopel S & Rorsman P (1999). CaM kinase II-dependent mobilization of secretory granules underlies acetylcholine-induced stimulation of exocytosis in mouse pancreatic B-cells. *J Physiol* **518**, 745–759.

Grynkiewicz G, Poenie M & Tsien RY (1985). A new generation of Ca^{2+} indicators with greatly improved fluorescence properties. *J Biol Chem* **260**, 3440–3450.

Gylfe E (1977). Serotonin as marker for the secretory granules in the pancreatic β-cell. *Acta Physiol Scand* Suppl **452**, 125–128.

Gylfe E (1978). Association between 5-hydroxytryptamine release and insulin secretion. *J Endocrinol* **78**, 239–248.

Henquin JC (2000). Triggering and amplifying pathways of regulation of insulin secretion by glucose. *Diabetes* **49**, 1751–1760.

Holst JJ (1997). Enteroglucagon. *Ann Rev Physiol* **59**, 257–271.

Holz GG & Habener JF (1992). Signal transduction crosstalk in the endocrine system: pancreatic β-cells and the glucose competence concept. *Trends Biochem Sci* **17**, 388–393.

Holz GG, Kuhtreiber WM & Habener JF (1993). Pancreatic β-cells are rendered glucose competent by the insulinotropic hormone glucagon-like peptide-1-(7–37). *Nature* **361**, 362–365.

Holz GG, Leech CA, Heller RS, Castonguay M & Habener JF (1999). cAMP-dependent mobilization of intracellular Ca^{2+} stores by activation of ryanodine receptors in pancreatic β-cells. A Ca^{2+} signaling system stimulated by the insulinotropic hormone glucagon-like peptide-1-(7–37). *J Biol Chem* **274**, 14147–14156.

Islam MS (2002). The ryanodine receptor calcium channel of beta-cells: molecular regulation and physiological significance. *Diabetes* **51**, 1299–1309.

Islam MS, Leibiger I, Leibiger B, Rossi D, Sorrentino V, Ekstrom TJ, Westerblad H, Andrade FH & Berggren PO (1998). In situ activation of the type 2 ryanodine receptor in pancreatic β-cells requires cAMP-dependent phosphorylation. *Proc Natl Acad Sci U S A* **95**, 6145–6150.

Islam MS, Rorsman P & Berggren PO (1992). Ca^{2+}-induced Ca^{2+} release in insulin-secreting cells. *FEBS Lett* **296**, 287–291.

Kang G, Chepurny OG & Holz GG (2001*a*). cAMP-regulated guanine nucleotide exchange factor-II (Epac2). mediates Ca^{2+}-induced Ca^{2+} release in INS-1 pancreatic β-cells. *J Physiol* **536**, 375–385.

Kang G, Chepurny OG & Holz GG (2001*b*). cAMP-dependent Ca^{2+}-induced Ca^{2+} release (CICR). triggers exocytosis and endocytosis in pancreatic β-cells. *Biophys J* **80**, 136A.

Kang G & Holz GG (2000). Functional coupling of intracellular Ca^{2+} stores to exocytosis of insulin in pancreatic β-cells. *Biophys J* **78**, 146A.

Kang G & Holz GG (2002). Dual signaling capacity of Ca^{2+}-induced Ca^{2+} release as a stimulus for exocytosis and endocytosis in INS-1 pancreatic β-cells. *Biophys J* **82**, 615A.

Kasai H, Suzuki T, Liu T, Kishimoto T & Takahashi N (2002). Fast and cAMP-sensitive mode of Ca^{2+}-dependent exocytosis in pancreatic β-cells. *Diabetes* **51**, S19–24.

Kashima Y, Miki T, Shibasaki T, Ozaki N, Miyazaki M, Yano H & Seino S (2001). Critical Role of cAMP-GEFII-Rim2 complex in incretin-potentiated insulin secretion. *J Biol Chem* **276**, 46046–46053.

Kennedy ED, Rizzuto R, Theler JM, Pralong WF, Bastianutto C, Pozzan T & Wollheim CB (1996). Glucose-stimulated insulin secretion correlates with changes in mitochondrial and cytosolic Ca^{2+} in aequorin-expressing INS-1 cells. *J Clin Invest* **98**, 2524–2538.

Leech CA, Holz GG, Chepurny O & Habener JF (2000). Expression of cAMP-regulated guanine nucleotide exchange factors in pancreatic β-cells. *Biochem Biophys Res Commun* **278**, 44–47.

Leech CA, Holz GG & Habener JF (1994). Voltage-independent calcium channels mediate slow oscillations of cytosolic calcium that are glucose dependent in pancreatic β-cells. *Endocrinology* **135**, 365–372.

Lemmens R, Larsson O, Berggren PO & Islam MS (2001). Ca^{2+}-induced Ca^{2+} release from the endoplasmic reticulum amplifies the Ca^{2+} signal mediated by activation of voltage-gated L-type Ca^{2+} channels in pancreatic β-cells. *J Biol Chem* **276**, 9971–9977.

Lindstrom P, Norlund L, Sehlin J & Taljedal IB (1984). Effects of 5-hydroxytryptamine on rubidium ion fluxes and insulin release in cultured pancreatic islets. *Endocrinology* **115**, 2121–2125.

Lindstrom P, Sehlin J & Taljedal IB (1980). Characteristics of 5-hydroxytryptamine transport in pancreatic islets. *Br J Pharmacol* **68**, 773–778.

Llinas R, Sugimori M & Silver RB (1995). The concept of calcium concentration microdomains in synaptic transmission. *Neuropharmacology* **34**, 1443–1451.

Maechler P, Kennedy ED, Sebo E, Valeva A, Pozzan T & Wollheim CB (1999). Secretagogues modulate the calcium concentration in the endoplasmic reticulum of insulin-secreting cells. Studies in aequorin-expressing intact and permeabilized INS-1 cells. *J Biol Chem* **274**, 12583–12592.

Mears D, Leighton X, Atwater I & Rojas E (1999). Tetracaine stimulates insulin secretion from the pancreatic β-cell by release of intracellular calcium. *Cell Calcium* **25**, 59–68.

Mitchell KJ, Pinton P, Varadi A, Tacchetti C, Ainscow EK, Pozzan T, Rizzuto R & Rutter GA (2001). Dense core secretory vesicles revealed as a dynamic Ca^{2+} store in neuroendocrine cells with a vesicle-associated membrane protein aequorin chimaera. *J Cell Biol* **155**, 41–51.

Nakagaki I, Sasaki S, Hori S & Kondo H (2000). Ca^{2+} and electrolyte mobilization following agonist application to the pancreatic β cell line HIT. *Pflugers Arch* **440**, 828–834.

Narita K, Akita T, Hachisuka J, Huang S, Ochi K & Kuba K (2000). Functional coupling of Ca^{2+} channels to ryanodine receptors at presynaptic terminals. Amplification of exocytosis and plasticity. *J Gen Physiol* **115**, 519–532.

Ohara-Imaizumi M, Nakamichi Y, Tanaka T, Ishida H & Nagamatsu S (2002). Imaging exocytosis of single insulin secretory granules with evanescent wave microscopy: distinct behavior of granule motion in biphasic insulin release. *J Biol Chem* **277**, 3805–3808.

Ozaki N, Shibasaki T, Kashima Y, Miki T, Takahashi K, Ueno H, Sunaga Y, Yano H, Matsuura Y, Iwanaga T, Takai Y & Seino S (2000). cAMP-GEFII is a direct target of cAMP in regulated exocytosis. *Nat Cell Biol* **2**, 805–811.

Pouli AE, Emmanouilidou E, Zhao C, Wasmeier C, Hutton JC & Rutter GA (1998). Secretory-granule dynamics visualized *in vivo* with a phogrin-green fluorescent protein chimaera. *Biochem J* **333**, 193–199.

Prentki M & Matschinsky FM (1987). Ca^{2+}, cAMP, and phospholipid-derived messengers in coupling mechanisms of insulin secretion. *Physiol Review* **67**, 1185–1248.

Qian WJ & Kennedy RT (2001). Spatial organization of Ca^{2+} entry and exocytosis in mouse pancreatic β-cells. *Biochem Biophys Res Commun* **286**, 315–321.

Renstrom E, Eliasson L & Rorsman P (1997). Protein kinase A-dependent and -independent stimulation of exocytosis by cAMP in mouse pancreatic B-cells. *J Physiol* **502**, 105–118.

Scheenen WJ, Wollheim CB, Pozzan T & Fasolato C (1998). Ca^{2+} depletion from granules inhibits exocytosis. A study with insulin-secreting cells. *J Biol Chem* **273**, 19002–19008.

Schulte A & Chow RH (1996). A simple method for insulating carbon-fiber microelectrodes using anodic electrophoretic deposition of paint. *Anal Chem* **68**, 3054 –3058.

Skoglund G, Hussain MA & Holz GG (2000). Glucagon-like peptide-1 stimulates insulin gene promoter activity by protein kinase A-independent activation of the rat insulin I gene cAMP response element. *Diabetes* **49**, 1156–1164.

Smith C, Moser T, Xu T & Neher E (1998). Cytosolic Ca^{2+} acts by two separate pathways to modulate the supply of release-competent vesicles in chromaffin cells. *Neuron* **20**, 1243–1253.

Smith PA, Duchen MR & Ashcroft FM (1995). A fluorimetric and amperometric study of calcium and secretion in isolated mouse pancreatic β-cells. *Pflugers Arch* **430**, 808–818.

Smith PA, Proks P & Ashcroft FM (1999). Quantal analysis of 5-hydroxytryptamine release from mouse pancreatic β-cells. *J Physiol* **521**, 651–664.

Takahashi N, Kadowaki T, Yazaki Y, Ellis-Davies GC, Miyashita Y & Kasai H (1999). Post-priming actions of ATP on Ca^{2+}-dependent exocytosis in pancreatic β-cells. *Proc Natl Acad Sci U S A* **96**, 760–765.

Tsuboi T, Zhao C, Terakawa S & Rutter GA (2000). Simultaneous evanescent wave imaging of insulin vesicle membrane and cargo during a single exocytotic event. *Curr Biol* **10**, 1307–1310.

Varadi A & Rutter GA (2002). Dynamic imaging of endoplasmic reticulum Ca^{2+} concentration in insulin-secreting MIN6 cells using recombinant targeted cameleons: roles of sarco(endo)plasmic reticulum Ca^{2+}-ATPase (SERCA)-2 and ryanodine receptors. *Diabetes* **51**, S190–201.

von Ruden L & Neher E (1993). A Ca-dependent early step in the release of catecholamines from adrenal chromaffin cells. *Science* **262**, 1061–1065.

Willmott NJ, Galione A & Smith PA (1995). Nitric oxide induces intracellular Ca^{2+}mobilization and increases secretion of incorporated 5-hydroxytryptamine in rat pancreatic β-cells. *FEBS Lett* **371**, 99–104.

Wollheim CB & Sharp GW (1981). Regulation of insulin release by calcium. *Physiol Rev* **61**, 914–973.

Xu GG, Gao ZY, Borge PD Jr & Wolf BA (1999). Insulin receptor substrate 1-induced inhibition of endoplasmic reticulum Ca^{2+} uptake in β-cells. Autocrine regulation of intracellular Ca^{2+} homeostasis and insulin secretion. *J Biol Chem* **274**, 18067–18074.

Zawalich WS, Tesz GJ & Zawalich KC (2001). Are 5-hydroxytryptamine-preloaded β-cells an appropriate physiologic model system for establishing that insulin stimulates insulin secretion? *J Biol Chem* **276**, 37120–37123.

Acknowledgements

G.G.H. acknowledges the support of the National Institutes of Health (DK-45817, DK-52166) and the American Diabetes Association (Research Grant Award).